

Reactions of Charged Substrates. 7. The Methoxymethyl Carbenium Ion Problem. 2. A Semiempirical Study of the Kinetic and Thermodynamic Stabilities of Linear and Cyclic Oxo- and Thiocarbenium Ions Generated from Aldehyde Hydrates, Hemiacetals, Acetals, and Methyl Ribosides and Glucosides

Neil Buckley* and Norman J. Oppenheimer

The Department of Pharmaceutical Chemistry, S-926, Box 0446, The University of California, San Francisco, California 94143-0446

Received April 24, 1996[®]

Factors affecting the cleavage of the carbon–oxygen bond in linear and cyclic aldehyde hydrates, hemiacetals, acetals, and methyl ribosides and glucosides have been investigated using semiempirical calculations (AM1 and PM3). (For some systems, low- and high-level *ab initio* energies are available for comparison with the semiempirical results. With one exception, the results obtained by the two methods show excellent agreement in relative energies and trends in reactivity.) The effects on reactivity and stability caused by substituting a sulfur for the α oxygen in the oxocarbenium ion were also studied. In general, systems that can have an antiperiplanar alignment of lone pairs on the leaving group and potential oxocarbenium ion oxygens undergo spontaneous cleavage. An examination of various conformers of the leaving group relative to the potential oxocarbenium oxygen shows, however, that lone pair repulsion and steric factors for MeOH as the leaving group are more important than the antiperiplanar effect for bond cleavage. All compounds in which the α -oxygen in the potential carbenium ion is replaced by sulfur undergo spontaneous cleavage regardless of the leaving group or structure of the compound. Energy profiles, ΔF^\ddagger , and ΔH_R values show that linear and cyclic thiocarbenium ions are much more stable than the corresponding oxocarbenium ions. Comparison of results for methyl ribosides and glucosides with results for corresponding pyridinium substrates suggests that both should hydrolyze through an A-1 mechanism. General-acid catalysis with hydronium as the acid was studied. With solution results, the computations suggest that substrates with either a good leaving group or stable oxocarbenium ion react with rate-limiting proton transfer from the acid to the leaving group but that substrates with both a good leaving group and stable carbenium ion react with concerted proton transfer and bond cleavage.

Introduction

There is substantial evidence that the specific-acid catalyzed hydrolysis of acetals, ketals, and orthoesters occurs by an A-1 mechanism (Scheme 1).¹ General acid catalysis is observed only for substrates with good leaving groups and potentially stable oxocarbenium ions (1-(aryloxy)tetrahydrofurans [THF-OAr]² and -tetrahydropyrans [THP-OAr]³) or exceedingly stable carbenium ions (tropone diethyl ketal,⁴ and dioxolane hemi⁵ and ortho esters⁶). Acetals and ketals formed from "ordinary" carbonyl compounds and weakly basic aliphatic alcohols do not undergo general-acid catalysis.¹ THF- and THP-OAr substrates with electron-withdrawing groups on the phenol undergo pH-independent "spontaneous" bond

* To whom correspondence should be addressed. Phone: (707) 824-9770. Fax: (415) 476-9687. E-mail: buckley@sonic.net.

[®] Abstract published in *Advance ACS Abstracts*, October 15, 1996.

(1) Leading and recent reviews: (a) Capon, B. *Chem. Rev.* **1969**, *69*, 407–498. (b) Cordes, E. H.; Bull, H. G. *Chem. Rev.* **1973**, *73*, 581–603. (c) Sinnott, M. L. In *The Chemistry of Enzyme Action*; Page, M. L., Ed.; Elsevier: Amsterdam, 1984; pp 389–431.

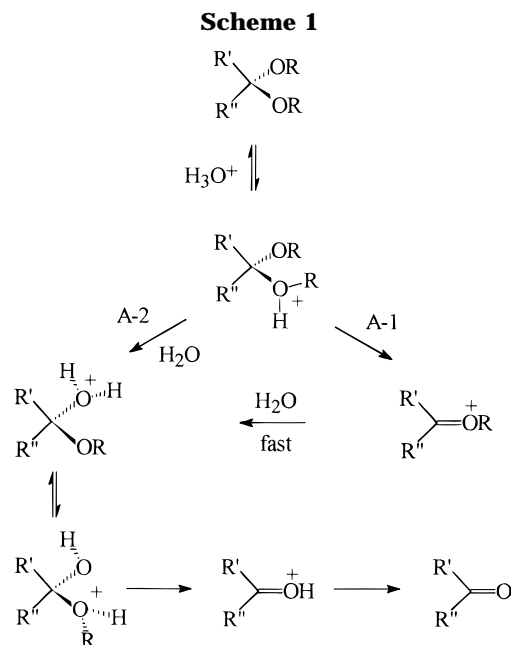
(2) Lönnberg, H.; Poljola, V. *Acta Chem. Scand. A* **1976**, *30*, 669–670.

(3) Fife, T. H.; Jao, L. K. *J. Am. Chem. Soc.* **1968**, *90*, 4081–4085. Fife, T. H.; Brod, L. H. *J. Am. Chem. Soc.* **1970**, *92*, 1681–1684. Craze, G.-A.; Kirby, A. J. *J. Chem. Soc., Perkin Trans. 2* **1978**, 354–356.

(4) Anderson, E.; Fife, T. H. *J. Am. Chem. Soc.* **1969**, *91*, 7163–7166.

(5) Ahmad, M.; Bergstrom, R. G.; Cashen, M. J.; Chiang, Y.; Kresge, A. J.; McClelland, R. A.; Powell, M. F. *J. Am. Chem. Soc.* **1979**, *101*, 2669–2677.

(6) Chiang, Y.; Kresge, A. J.; Salomaa, P.; Young, C. I. *J. Am. Chem. Soc.* **1974**, *96*, 4494–4499.



cleavage,^{2,3} and [(methoxymethyl)aryl]oxy substrates undergo nucleophilic substitution reactions.^{7,8} Methyl glucopyranosides do not undergo general-acid catalysis, which has caused somewhat of a dilemma because the

(7) Knier, B. L.; Jencks, W. P. *J. Am. Chem. Soc.* **1980**, *102*, 6789–6798.

glycosyl bond in polysaccharides is cleaved readily by lysozyme, which must act through general-acid catalysis.^{1a}

As part of our computational study of the gas-phase dissociation of charged benzyl substrates,⁸ we attempted to minimize (in AM1 and PM3) the ground states for protonated benzyl alcohols bearing 4-substituents (O⁻, OH, MeO, NH₂, NMeH, NMe₂, SH, SMe, Me, H, Cl, NO₂). The methylene-oxygen bond underwent spontaneous cleavage upon minimization in all substrates except the 4-nitro compound. There is a precedent for this reaction in the literature. Ichikawa and Harrison⁹ found that there is essentially complete dissociation of the methylene-oxygen bond in the chemical ionization spectra (methane or ammonia reagent gases) of substituted benzyl alcohols. (There is a second reaction in which ring-protonated substrate expels formaldehyde.) A similar computational result has been reported by Schröder et al.,¹⁰ who found that addition of an oxygen (or nitrogen) to a cationic center in simple aliphatic systems can increase the PM3-calculated gas-phase stabilization energies by significant amounts and can lead to spontaneous bond cleavage. Replacement of a methyl group in Me₃O⁺ with MeOCH₂⁻ led to spontaneous cleavage of a carbon-oxygen bond to liberate Me₂O. Bond cleavage in the (methoxymethyl)dimethyloxonium is 46.5 kcal/mol more exothermic than cleavage of the trimethyloxonium, and [MeO=CH₂]⁺ is 91.4 kcal/mol more stable than the methyl cation. Caserio found that cyclic ortho esters with oxonium leaving groups dissociate rapidly and completely in the gas phase.¹¹ Thus, the driving force is the stability of the products, and the reaction occurs with a small or no barrier. In initial studies on cyclic systems, we found that minimization of protonated cyclopentanol in AM1 or PM3 did not lead to bond cleavage. Upon minimization of the protonated α-oxygen homolog (the cyclic hemiacetal of 4-hydroxybutanal [**13a**]), however, the bond length of the reaction coordinate increased spontaneously from 1.58 to 2.78 Å; to obtain Δ*H*_f for the ground state, it was necessary to constrain the C-O bond. The cyclic oxocarbenium ion is 5.5 kcal/mol more stable than the cyclic aliphatic carbenium ion.

This suggested that a relatively simple “yes-no” computational test for relative stabilities might be obtained merely by attempting to minimize protonated forms of various substrates. In the event, the situation is much more complex: cleavage of the C-O bond depends on the leaving group, leaving group conformations, anomeric effects, substituent effects, and the stability of the resulting carbenium ions. Results for the protonated oxygen substrates reported here generally parallel those found for the corresponding pyridinium substrates reported in the preceding paper,¹² with a few notable exceptions.

Methods

Computations. The semiempirical methods reported in the preceding paper were used here.¹² For the THF, THP, and sugar substrates, the various conformations were set

(8) Buckley, N.; Maltby, D.; Burlingame, A. L.; Oppenheimer, N. J. *J. Org. Chem.* **1996**, *61*, 2753–2762.

(9) Ichikawa, H.; Harrison, A. G. *Org. Mass. Spectrom.* **1978**, *13*, 389–396.

(10) Schröder, S.; Buckley, N.; Oppenheimer, N. J.; Kollman, P. A. *J. Am. Chem. Soc.* **1992**, *114*, 8231–8238.

(11) Caserio, M. C.; Souma, Y.; Kim, J. K. *J. Am. Chem. Soc.* **1981**, *103*, 6712–6716.

(12) Buckley, N.; Oppenheimer, N. J. *J. Org. Chem.* **1996**, *61*, 8039.

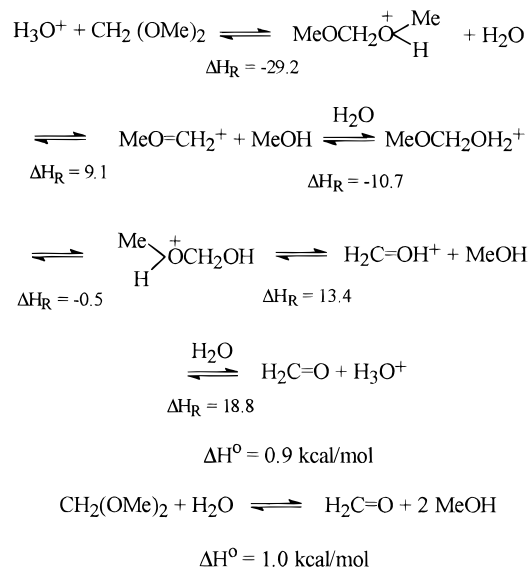


Figure 1. Step wise mechanism for the specific-acid-catalyzed hydrolysis of formaldehyde methyl acetal. Δ*H*_R for each step is ΣΔ*H*_f [products] – ΣΔ*H*_f [reactants]; Δ*H*^o is the sum of Δ*H*_R for each step. The value of Δ*H*^o for the stepwise mechanism (10 catalysts, products, and/or reactants) is within 0.1 kcal/mol of Δ*H*^o obtained considering only reactants and products.

manually and minimized. Succeeding conformations were set by rotating the protonated leaving group 60°. The same relative orientation of the proton and lone pairs, designated as *i-vi* for the six principal conformations, were used consistently for the structures shown in the figures and charts. For the studies of general-acid catalysis, the O-H-O bond between substrate LG and acid was constrained to 180°.

Controls. For several of the systems studied here, *ab initio* values are available that can be compared with the semiempirical energies. They are discussed at the appropriate place. In general, there is good agreement among the results obtained by the two methods; certainly the trends in *relative* energies and *relative* stabilities obtained with semiempirical and *ab initio* methods agree.

As a further check on the internal consistency of the semiempirical method, we calculated the starting, intermediate, and final structures in a six-step mechanism for the specific-acid-catalyzed hydrolysis of formaldehyde dimethyl acetal and compared the overall Δ*H*^o obtained for each step with the value obtained by considering only the initial and final products (Figure 1). The value of Δ*H*^o obtained by summing the values of Δ*H*_R for each reaction in the stepwise mechanism is 0.1 kcal/mol lower than the value obtained considering the initial and final products, which is excellent agreement considering the possible error for each step and the fact that the absolute energies were rounded off to the nearest 0.1 kcal/mol. This agreement shows that the method is internally consistent and that numbers may be compared between and among series.

Results and Discussion

Linear Compounds. (a) Formaldehyde Hydrate.

The simplest member of the series of linear compounds studied is formaldehyde hydrate, CH₂(OH)₂ (**1**). Wipff¹³ has reported low-level *ab initio* energies (at the 4-31G level) for ground-state and protonated forms of several conformations of **1**. The PM3 energies for the ground-state rotomers **1A–D** show the same trend in relative energies reported by Wipff, although the PM3 energies are lower by a factor of 2 (Figure 2); the structures and energies mirror the trends found for CH₂(OMe)₂ by

(13) Wipff, G. *Tetrahedron Lett.* **1978**, 3269–3270.

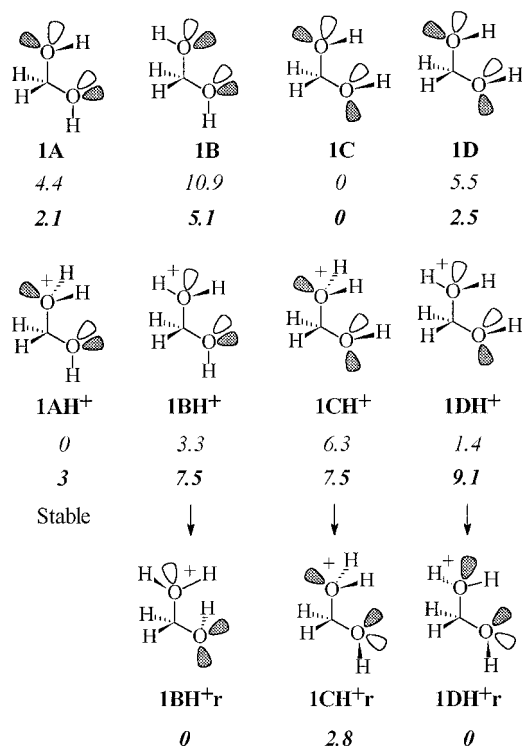
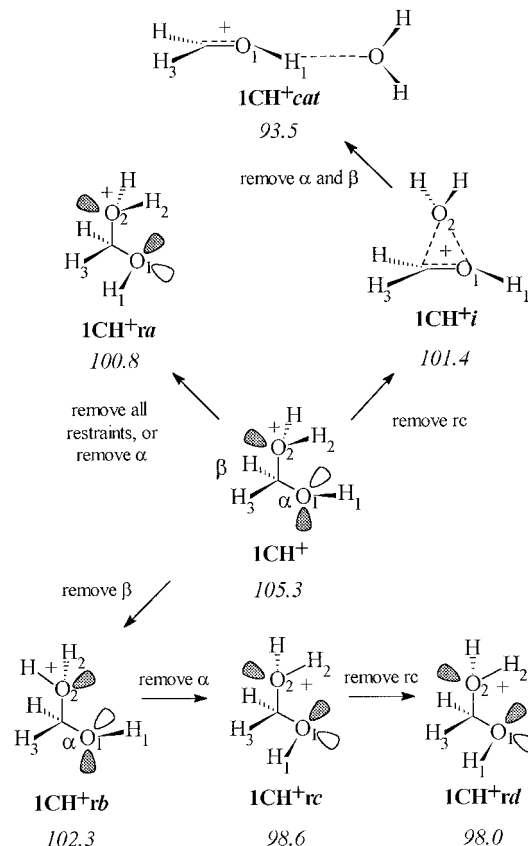


Figure 2. Structures and energies for formaldehyde hydrate (**1**). The unprotonated structures **1A–D** are those considered by Wipff¹³ and calculated at the 4-31G level of theory with *ab initio* methods (relative energies in italics); the PM3 values obtained in this study are given in bold face italic. Upon full PM3 minimization with no constraints, three of the protonated forms, **1BH⁺–1DH⁺** revert to much more stable rotomers **1BH⁺r–1DH⁺r**. **1AH⁺** is stable.

Andrews et al.¹⁴ that are discussed below (see Figure 9). The PM3 energies for the protonated forms **1AH⁺–1DH⁺**, with torsional angles constrained to reproduce Wipff's structures, show the same trends in relative energies he reported, but PM3 minimization of the unrestricted forms **1BH⁺–1DH⁺** lead to more stable forms **1BH⁺r–1DH⁺r** (Figure 2) that reflect the stabilizing $n\sigma^*$ interactions within the structures emphasized by Andrews et al.¹⁴ for the dimethoxy series.

The complexity of this relatively simple system can be appreciated from the various local minima that can be obtained from **1CH⁺** (Figure 3). The initial structure has a staggered conformation (viewed along the O_2 –C bond) obtained by constraining the H_3 –C– O_1 – H_1 bond angle α and the H_3 –C– O_2 – H_2 bond angle β to 60° and restraining the C– O_2 bond—the reaction coordinate—to 1.61 Å, the reaction coordinate distance in PM3 structures for **1AH⁺–1DH⁺**; after full minimization, $\Delta H_f = 105.3$ kcal/mol. Removal of all restraints, or of the torsional angle α , followed by minimization gives **1CH⁺ra**, in which the O_1 hydroxyl has rotated by 60° to introduce two stabilizing $n\sigma^*$ interactions; this minor change in structure is worth 4.5 kcal/mol in energy of stabilization. If only the restraint on the reaction coordinate is removed for **1CH⁺**, spontaneous bond cleavage occurs to **1CH⁺i** because of the antiperiplanar orbitals in **1CH⁺**. (Note that in the first case, rotation removes the antiperiplanar interaction and prevents bond cleavage.) It is interesting that the stable ion–



H_3 –C– O_1 – H_1 torsional angle = $60^\circ = \alpha$
 H_3 –C– O_2 – H_2 torsional angle = $60^\circ = \beta$
 rc = reaction coordinate = C– O_2 bond

Figure 3. Various structures obtained upon full PM3 minimization of **1CH⁺** by stepwise removal of the torsional angle restraints α and β and the reaction coordinate. Each restraint was held at a force constant of 10^3 . The numbers in italics are the absolute PM3 ΔH_f for each structure.

dipole complex **1CH⁺i** has a symmetrical bridged structure—C– O_2 and O_1 – O_2 bond length = 2.72 Å and O_1 –C– O_2 and C– O_1 – O_2 bond angles = 76° —not unlike phenonium ions, which is very similar to ion–dipole complexes obtained for several pyridinium compounds reported in the companion paper.¹² While the ion–dipole complex is 3.9 kcal/mol more stable than the structure from which it was generated, it is 3.4 kcal/mol less stable than the most stable rotomer **1CH⁺rd**. **1CH⁺i**, however, is an intermediate; removal of the α and β torsional angle restraints followed by minimization leads to the planar oxocarbenium ion **1CH⁺cat** in which the departed water is hydrogen bonded to the O_1 hydroxyl. This is the most stable structure found in this series ($\Delta H_f = 93.5$ kcal/mol).

These structures are reproduced if the rc bond length is increased in 0.1 Å steps from the initial structure in which the torsional angle restraints have been removed; the complete energy profile is shown in Figure 4. A small change in the rc (0.04 Å) leads to a large stabilization in energy to point A; increasing the bond length leads to B. The transition from B to C in Figure 4 represents inversion of the departing water hydrogens from syn to O_1 to anti. Further increases in the bond length lead to point D, which is the bridged structure **1CH⁺i** (Figure 3). A 0.1 Å change in reaction coordinate bond length leads to a precipitous drop in energy caused by the

(14) Andrews, C. W.; Bowen, J. P.; Fraser-Reid, B. *J. Chem. Soc., Chem. Commun.* **1989**, 1913–1916. These authors provide a review of earlier work.

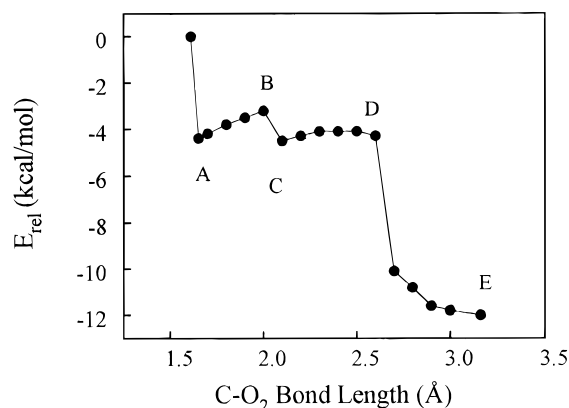


Figure 4. Full PM3 energy profile for minimization of 1CH^+ after removal of the restraint on the reaction coordinate. The reaction coordinate bond length was increased in 0.1 Å steps, and each structure was fully minimized. The transition A \rightarrow B represents the energy associated with an increase in the reaction coordinate bond length; B \rightarrow C represents a simple umbrella inversion of the protons on the leaving group oxygen; C \rightarrow D represents a change from a structure in which the C–O₂ bond is perpendicular to the plane of the insipient oxocarbenium ion to the symmetrical bridged structure 1CH^+i (Figure 3); D \rightarrow E represents the “folding over” of the departing water with formation of a hydrogen bond, eventually yielding the structure 1CH^+cat .

formation of a hydrogen bond between the departing water and the O₁-hydroxyl (H₁) to give a structure that eventually minimizes to 1CH^+cat . Thus, an initial structure in which there are antiperiplanar orbitals can collapse to the oxocarbenium ion with which the LG is still associated, although not in a position to return easily to either the intermediate or the ground-state structure.

Collapse need not occur, however. If the antiperiplanar orbital interaction is eliminated by removal of the constraint on the torsional angle β , full minimization yields structure 1CH^+rb in which the O₂-protonated hydroxyl has rotated to form a second staggered rotomer that adds two $n\sigma^*$ interactions and removes the antiperiplanar interaction, worth 3.1 kcal/mol (Figure 3). (Note that removal of the restraint on the reaction coordinate in this structure followed by minimization increases the reaction coordinate bond length to 1.74 Å without catastrophic bond cleavage and increases the stability by 0.2 kcal/mol, presumably because a repulsion between orthogonal lone pairs on O₁ and O₂ is reduced.) Removal of the α torsional angle from 1CH^+rb followed by full minimization causes both O₁ and O₂ hydroxyls to rotate to give 1CH^+rc , a maneuver that produces three $n\sigma^*$ interactions and removes the orthogonal repulsion, worth 3.7 kcal/mol relative to 1CH^+rb and 6.7 kcal/mol relative to the starting structure 1CH^+ . Finally, removing the rc restraint from this structure and minimizing gives 1CH^+rd , in which the rc bond length decreases to 1.57 Å and the energy is lowered by 0.6 kcal/mol, presumably by increasing the O₂–C–H $n\sigma^*$ interaction.

The wide range of structures with different energies that can be obtained by relatively minor stepwise alterations in geometry of this simple molecule shows the complexity inherent in the general system. As we show below, changes in the LG (from OH₂ to MeOH, say) or the heteroatom (from O to S) can affect the reactivity and the reaction profiles drastically.

(b) Formaldehyde Methyl Hemiacetal (2). Jeffery et al.¹⁵ have reported the *ab initio* (HF/4-31G) ground-

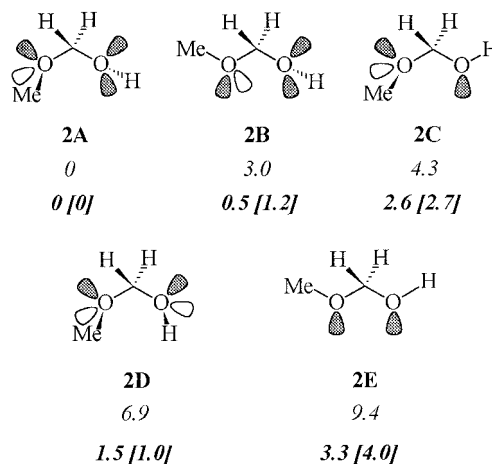


Figure 5. Structures and energies for formaldehyde methyl hemiacetal (**2**). The numbers in italics are the relative energies (in kcal/mol) calculated by Jeffery et al.¹⁵ at the HF/4-31G level of theory, with the torsional angles of the methoxy and hydroxyl restrained at 60° from the O–C–O plane. The numbers in boldface italic are PM3 relative energies calculated in this study, with the same restraints used by Jeffery et al. The numbers in brackets are PM3 energies obtained from full minimization after removal of the restraints; the basic conformations are retained, although the torsional angles change by as much as 22°.

state energies for various conformers of this compound in which the torsional angles of the MeO and OH groups are restrained to be 60° out of the O–C–O plane (Figure 5). In all but one instance (**2D**), the PM3 relative energies show the same trends, although they are lower than the HF/4-31G values as found above for **1**. If the restraints are released from the various conformers which are then fully minimized, the same relative energies are obtained; the differences are related to the change in torsional angle, by up to as much as 22°—from 60° to 38° for the MeO in **2A, C, D**, for example. We also found that **2C** minimizes to **2A** and **2E** minimizes to **2B** with the restraints released, which limits the stable PM3 structure to the three, similar to structures identified by Andrews et al.¹⁴ for formaldehyde dimethyl acetal (see Figure 9); these workers also found a similar trend in relative energies (see below).

There are two potential leaving groups for this compound. MeOCH₂OH₂⁺ (**3**) is 0.5 kcal/mol less stable than ⁺MeOHCH₂OH (**4**) in accord with the expected proton affinities. (Both structures were generated by restricting the respective C–O bond length to 1.56 Å and minimizing fully in PM3 to the most stable rotomer.) Protonation of either lone pair on the methoxy O produces the *R*- or *S*-form of **4**, both of which were examined.

Unlike the energy profiles for the pyridinium analogs reported in the companion paper,¹² the calculated stability of these compounds depends on the semiempirical method used. PM3-minimization of **3** leads to cleavage of the C–O bond for three rotomers (**3iv**–**3vi**), all of which are subject to orbital repulsion (Figure 6). The other rotomers are stable. AM1-minimization of **3** does not lead to bond cleavage for any rotomer, however. This difference is also reflected in the energy profiles (Figure 7). In PM3, **3i** has a small but distinct ΔH^\ddagger and forms an ion–dipole complex, while in AM1 there is no distinct

(15) Jeffery, G. A.; Pople, J. A.; Radom, L. *Carbohydr. Res.* **1974**, *38*, 81–95.

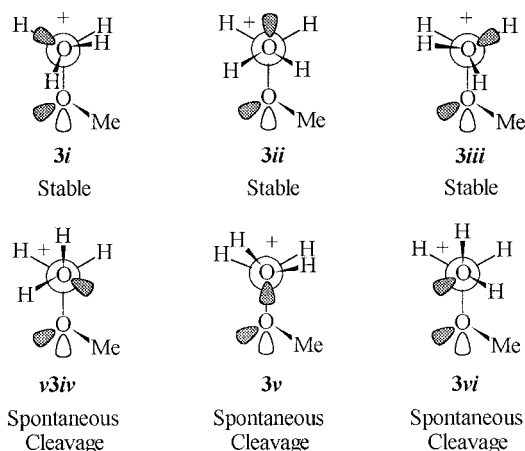


Figure 6. PM3 structures of 60° rotomers for protonation on the hydroxyl of 2. **4i–iii** are stable, **4iv–vi** undergo spontaneous cleavage upon minimization.

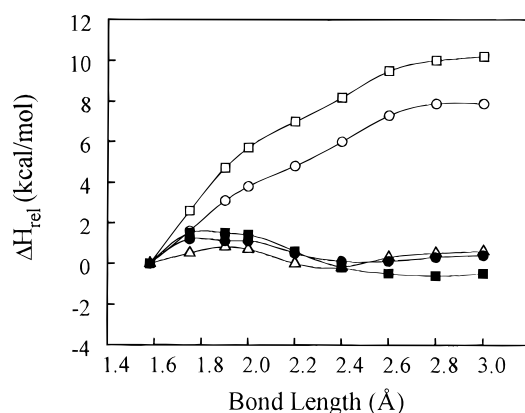
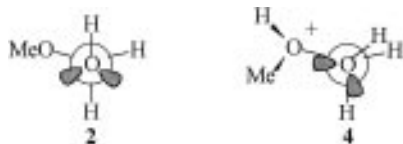


Figure 7. Energy profiles for dissociation of the C–O bond the most stable ground-state structures for **3** (○ = AM1; ● = PM3), **4** (□ = AM1; ■ = PM3), and **7** (△, AM1).

Chart 1



transition state, and the values of ΔH_R are high and positive (Table 1).

Protonation of either methoxy lone pair in **2** gives either the (*R*)- or (*S*)-form of **4** (Figure 8). The reactivity or stability of these conformers was analyzed by full PM3 minimization. Unlike the unprotonated conformers, in which the hydroxyl and methylene groups exist in a staggered conformation, in the protonated form the hydroxyl and methylene groups are eclipsed, a conformation that remains stable in all 12 rotomers considered (Chart 1). This conformation prevents an antiperiplanar alignment between the hydroxyl and methoxy orbitals in the protonated forms. The forms that undergo spontaneous cleavage upon minimization do so because of steric repulsion between the methoxy methyl and the hydroxyl in eclipsed conformers such as (*R*)-**4i** and (*S*)-**4iii** or by orbital repulsion as in (*R*)-**4vi** and (*S*)-**4iii**. It is interesting to compare (*R*)-**4vi** and (*S*)-**4vi** (Figure 8). Both have the extreme orbital repulsion caused by a gauche–gauche interaction between the methoxy orbital and the two orbitals on the hydroxyl. The gauche

Table 1. Semiempirical Enthalpies of Reaction (kcal/mol)

Compound	AM1	ΔH_R	PM3
MeOCH ₂ OH ₂ ⁺	21.1		10.0
MeOCH ₂ OHMe ⁺	22.8		8.5
MeOCHMeOH ₂ ⁺	12.5		2.6
MeOCHMeOHMe ⁺	11.5		0.4
MeSCH ₂ OH ₂ ⁺	-6.7		-7.8
MeSCH ₂ OHMe ⁺	-4.9		-7.5
MeSCHMeOH ₂ ⁺	-12.9		-10.5
MeSCHMeOHMe ⁺	-12.5		-12.7
		12.7	3.6
		12.6	0.6
		-14.4	-10.2
		-12.2	-15.6
		9.5	0.8
		4.7	-0.1
		6.9	-5.0
		7.9	-4.6
		-13.8	-12.0
		-15.7	-14.2
		-17.0	-16.5
		-18.4	-17.4

methoxy methyl–hydroxyl conformation in (*R*)-**4vi** causes spontaneous cleavage, but in (*S*)-**4vi**, in which the methoxymethyl and hydroxy are *trans*, minimization to the stable form (*S*)-**4i** occurs with relief of the orbital repulsion and no spontaneous cleavage. (The same situation occurs in the dimethoxy compound, as in (*R*)-**6aiv** (see Figures 10 and 11).) In (*S*)-**4iii**, there is only

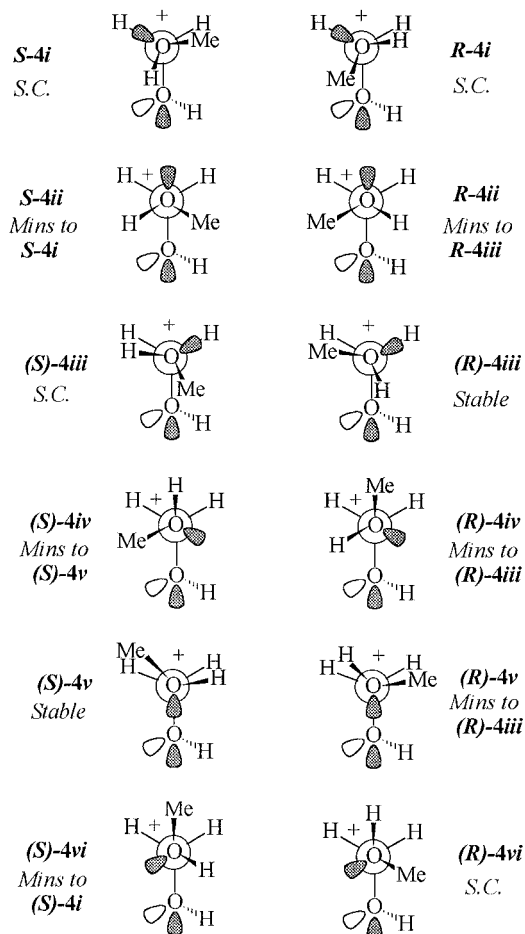


Figure 8. Twelve 60° chiral rotomers obtained by protonating the methoxy oxygen (0.5 kcal/mol more stable than the protonated hydroxyl form) of the most stable rotomer of **2**. The reactions are discussed in the text. *S.C.* = spontaneous cleavage; *Mins to* refers to the structure obtained on full PM3 minimization with no constraints.

steric repulsion between the methoxymethyl and the hydroxyl held in the eclipsed conformation. While a simple 60° rotation of the hydroxyl (to a staggered conformer) would produce an antiperiplanar alignment with the orbital of the methoxy oxygen that would satisfy the Deslongchamp criteria for bond scission,¹⁶ spontaneous cleavage occurs without a change in the geometry of the hydroxyl, which suggests in turn that steric repulsion is sufficient to cause cleavage. It should be noted, however, that the eclipsed conformation between the methylene and the hydroxyl may be the most stable form because it allows conjugation with the methylene carbon in the cation ($\text{H}_2\text{C}=\text{OH}^+$) without major geometric reorganization; it is also probably true that there is partial conjugation in the eclipsed ground-state conformers.

(c) Formaldehyde Dimethyl Acetal (5). Andrews et al.¹⁴ have performed *ab initio* computations on the neutral and protonated forms of this compound at a high level of theory (6-31G*). The most stable of the neutral forms have the geometries shown in Figure 9. The PM3 ΔH_f values parallel those of Andrews et al.¹⁴ and roughly match those for **4**.

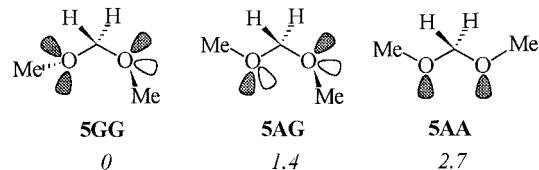


Figure 9. Three stable rotomers of **5**. The designations GG, AG, and AA are those used by Andrews et al.¹⁴ The numbers in italics are the relative PM3 ΔH_f in kcal/mol for the unconstrained structures.

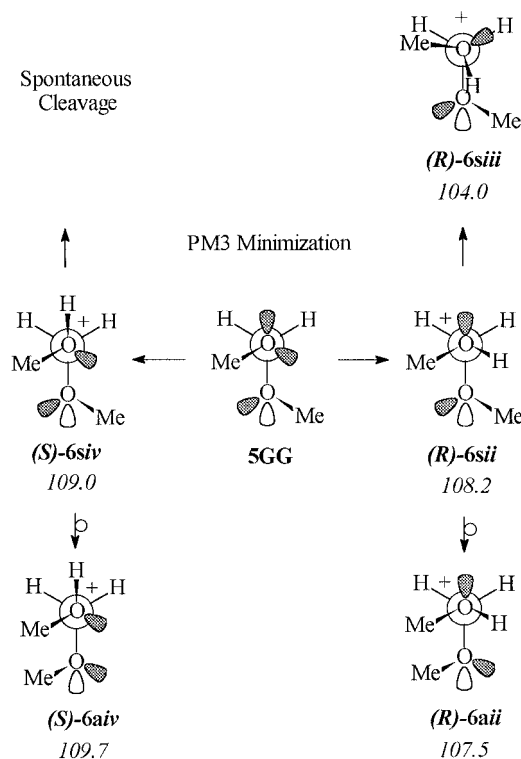


Figure 10. Two chiral forms obtained by protonation of either lone pair on the oxygen of **5GG**. In the numbering system for the forms, *s* refers to the methyl on the unprotonated methoxy being "syn" to the lone pair on the protonated methoxy, *a* as the methyl "anti" to the lone pair; italicized lower case Roman numerals refer to the rotomer in Figure 11. The italicized numbers are the absolute PM3 ΔH_f . See text for a description of the manipulations involved.

Protonation of the most stable conformer **5GG** on either lone pair leads to either (**S**)-**6siv** or (**R**)-**6sii** (Figure 10). The ΔH_f values obtained by full minimization of the constrained rotomers show that (**S**)-**6siv** is 0.8 kcal/mol less stable than (**R**)-**6sii**, presumably because of the orbital repulsion in (**S**)-**6siv**. When constraints are removed from (**S**)-**6siv** and (**R**)-**6sii** and both are fully minimized, (**S**)-**6siv** undergoes spontaneous cleavage, presumably because of an antiperiplanar alignment, while (**R**)-**6sii** minimizes to (**R**)-**6aii**, which is 4.2 kcal/mol more stable than (**R**)-**6sii**.

Rotation of the unprotonated methoxy into a gauche methyl–methyl interaction increases the energy of (**S**)-**6aiv** by 0.7 kcal/mol but decreases the energy of (**R**)-**6aii** by 0.7 kcal/mol. In the former case, methyl–methyl and lone pair–lone pair interactions are introduced, and a methyl–lone pair interaction is eliminated in the latter case, which suggests that the methyl–lone pair interaction is more important than the purely steric methyl–methyl gauche interaction.

(16) Deslongchamps, P. *Stereoelectronic Effects in Organic Chemistry*; Pergamon: New York, 1983; pp 30, 34–35. For the view in favor of these effects in these systems, see: Kirby, A. J. *Acc. Chem. Res.* **1984**, *17*, 305–311. For the view against, see: Hosie, L.; Marshall, P. J.; Sinnott, M. L. *J. Chem. Soc., Perkin Trans. 2* **1984**, 1121–1131.

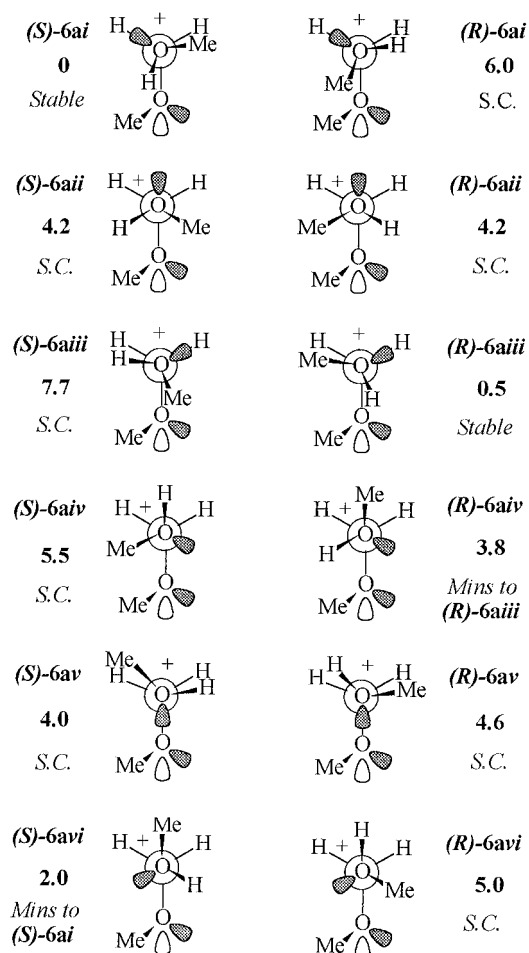
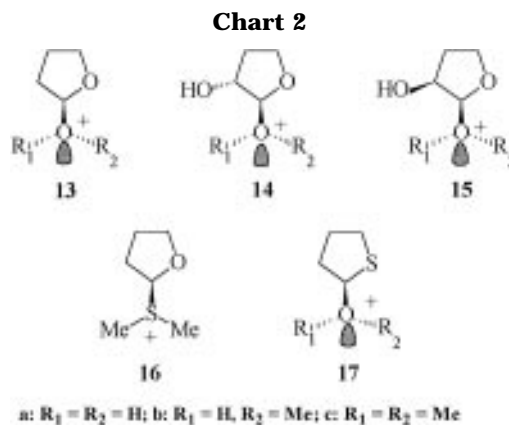


Figure 11. Twelve 60° chiral rotomers obtained by protonating the methoxy oxygen of the anti form of **6** (see legend to Figure 10 for explanation). The reactions are discussed in the text. The boldface numbers are the relative PM3 ΔH_f with torsional angle and reaction coordinate constraints used to hold the conformation. Note that the stability is a direct function of ΔH_R , which reflects either steric or orbital interactions. *S.C.* = spontaneous cleavage; *Mins to* refers to the structure obtained on full PM3 minimization with no constraints.

The reactivity of all 12 60° rotomers of (*S*)-**6a** and (*R*)-**6a** are shown in Figure 11; the relative energies of each rotomer are included. More rotomers in this series undergo spontaneous cleavage than do the protonated rotomers of the hemiacetal, which reflects the greater number of steric interactions present in the acetal rotomers. The basic pattern of reactivity is the same for the two series, however.

The energy profile for the acetal shows the same method dependence found for the hemiacetal. A distinct transition state is found only in PM3 (Figure 7). Thus, in the simple linear system, these effects are independent of the leaving group.

Replacing a proton on the aldehyde carbon with a methyl to give a secondary system affects the reactivity. Spontaneous bond cleavage occurred for all rotomers in MeOCHMeOH_2^+ (**7**) and MeOCMeCHOMeH^+ (**8**) in either AM1 or PM3. In PM3, **7** had a small but distinct transition state (Figure 7). The values of ΔH_R are 7.4 and 8.1 kcal/mol lower for **7** and **8** than for the corresponding primary systems (Table 1). With the exception of the conformation dependence, these result parallel



those found for dissociation of the corresponding pyridinium compounds.¹²

The effects of replacing an oxygen with a sulfur in the hemiacetal and acetal are dramatic. Minimization of $\text{MeSCH}_2\text{OH}_2^+$ (**9**) and $\text{MeSCH}_2\text{OHMe}^+$ (**10**) in AM1 and PM3 leads to cleavage of all rotomers, and the reactions are more exothermic by ca. 27 kcal/mol and ca. 17 kcal/mol in PM3 than for corresponding oxo compounds, respectively, which parallels the values for the pyridinium analogs reported in the companion paper.¹² In the PM3 energy profile for **9** (not shown), the ion-dipole complex has a relative energy of -16.3 kcal/mol and a C-OH₂ bond length of 3.2 Å. The change from a primary to a secondary system by the methyl-for-proton replacement in this series lowers ΔH_R by 2.7 kcal/mol for MeSCHMeOH_2^+ (**11**) and by 5.2 kcal/mol for MeSCHMeOHMe^+ (**12**) relative to the primary compounds. (A more general analysis of the effect of the sulfur for oxygen substitution is given below.)

Cyclic Compounds. (a) Five-Membered Rings. A number of THF and thio-THF systems were studied (Chart 2). Spontaneous bond cleavage depends on the conformation of the leaving group relative to the ring oxygen and on the leaving group.

Six conformations of **13a** were studied. All three staggered conformations (**13aii**, **13aiv**, and **13avi**, Figure 12) and one eclipsed (**13av**) cleaved spontaneously to an ion-dipole complex that is ca. 7 kcal/mol more stable than the ground-state structures (Table 1). Two of the eclipsed conformations (**13ai** and **13aiii**) were stable. Note that with the exception of **13aii**, this is the same pattern as seen for **6** and **16Eai-vi** in PM3. If the reaction coordinate bond is restrained, rotomers that cleave minimize to stable structures: **13aii** → **13ai**, **13av** → **13avi**, etc. Only one eclipsed conformation (**13biii**) was stable in **13b** (LG = MeOH), and no conformation was stable in **13c** (LG = Me₂O). Cleavage is apparently the result either of an appropriate antiperiplanar arrangement in the Deslongchamps scheme¹⁶ (**13aii**) or orbital repulsion (**13aiv**, **13av**, and **13avi**), neither of which is present in the stable structures (Chart 3). Differences between AM1 and PM3 are limited to cleavage of rotomers in conformation **ii**, which are stable in AM1 but cleave in PM3.

The energy profile for **13a** was generated by restraining the reaction coordinate bond to 1.57 Å (the length of the bond in stable structures) and minimizing the initial structure; **13ai** was obtained. In PM3, a distinct transition state ($\Delta H^\ddagger = 2$ kcal/mol) with a stable ion-dipole complex was obtained (Figure 13). Energy profiles for **13b** have no barrier to collapse with formation of a stable

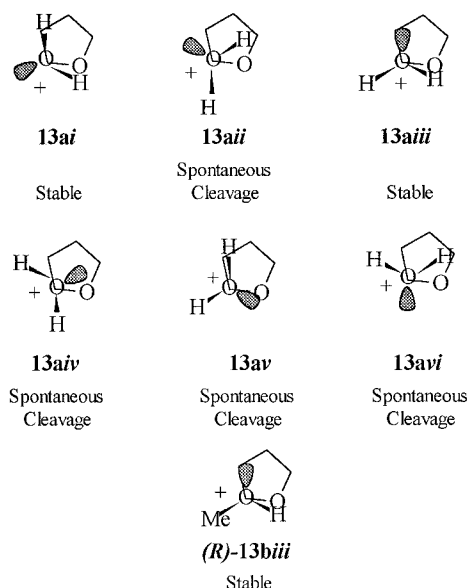


Figure 12. Six conformers for the protonated form of the cyclic hemiacetal of 4-hydroxybutanal, which show the same reactivity pattern found for **4** (see Figure 6), with the exception of **13aaii**, which cleaves upon minimization. All conformers of the (*R*)- and (*S*)-forms of **13b** cleave except **13bii**, and all conformers of **13c**, the dimethyloxonium salt, cleave.

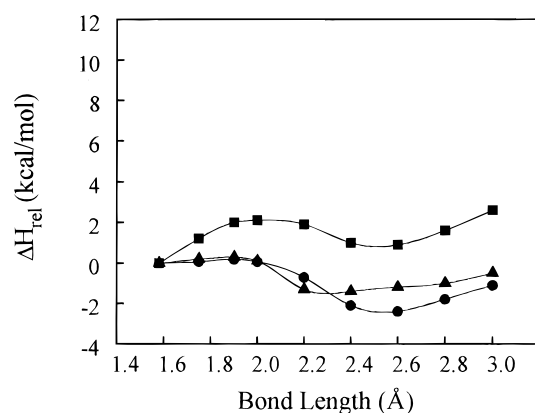
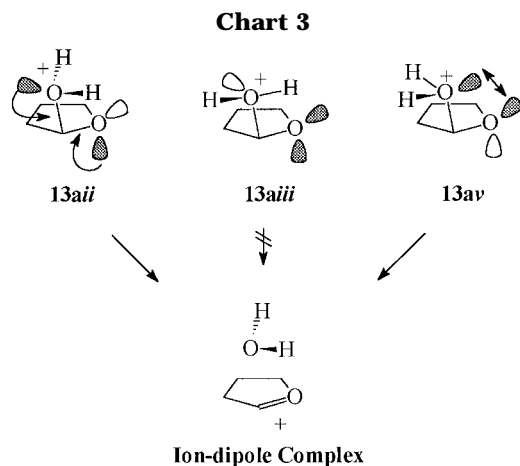


Figure 13. PM3 energy profiles for cleavage of **13ai** (■), **16Aa** (▲), and **16Ea** (●).



ion-dipole complex (not shown), which parallels the pattern for the deoxy methylribofuranoside discussed below.

As found for the corresponding pyridinium substrates,¹² the THF substrate has a higher ΔH^\ddagger (2.1 kcal/

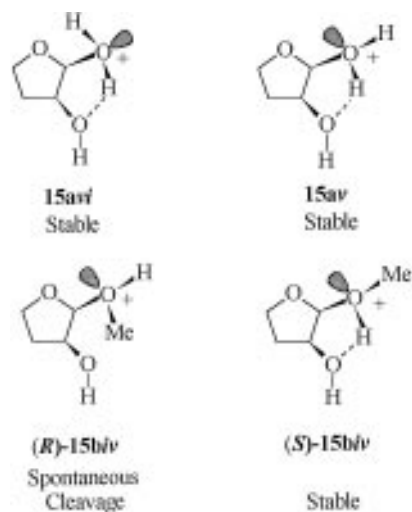


Figure 14. Effect of hydrogen bond formation on the stability of several conformers of **15**.

mol) than the THF substrates, in which the axial compound had a slightly higher (0.2 kcal/mol) ΔH^\ddagger than the equatorial compound (0.1 kcal/mol). Thus, the arguments given in the companion paper¹² in terms of activation values for the stabilities of the pyridinium compounds apply equally to the hydroxy compounds.

The *trans*-3-hydroxy compound **14** shows essentially the same pattern as found for **13**, despite the fact that the oxocarbenium ion would be destabilized by the inductive effect of the 3-hydroxy, which is analogous to the effect in β -nicotinamide ribosides.¹⁷ The *cis*-3-hydroxy compound **15**, however, shows a different pattern in which formation of a hydrogen bond between the protons on the 2-hydroxy and the oxygen of the 3-hydroxy stabilizes the structure and prevents spontaneous cleavage upon minimization. For instance, both **14avi** and **14av** (Figure 14) are stable structures, while the corresponding rotomers **14av** and **14avi** (Figure 12) undergo spontaneous cleavage upon PM3 minimization. The same pattern is seen in **15bvi**; the (*R*)-form, which will not form a hydrogen bond, undergoes spontaneous cleavage, while the (*S*)-form, which can form a hydrogen bond, is stable (although we cannot rule out steric repulsion in the former case).

Neither pyridine¹² nor dimethyl sulfide **16** is expelled upon minimization of the respective 2-THF derivatives. Water, methanol, and dimethyl ether are expelled spontaneously upon PM3 minimization of the MM2-minimized forms of thio-THF compounds **17a–c**, however. This suggests that the stability of the insipient carbenium ion or ion-dipole complex and not stereoelectronic or repulsive interactions is responsible for cleavage. Thus, the results for the five-membered systems parallel those found for the corresponding pyridinium compounds reported in the companion paper.¹²

(b) Six-Membered Rings. Several six-membered compounds were studied (Chart 4). The equatorial hemiacetal **16E** showed essentially the same conformational dependence seen for **2** (Figure 6) and **15** (Figure 12). Some forms minimized to stable forms by simple rotation of the leaving group (Figure 15). Simultaneously, the geometry around the anomeric carbon was flattening; if the minimization was stopped and the

(17) Buckley, N.; Handlon, A. L.; Maltby, D.; Burlingame, A. L.; Oppenheimer, N. J. *J. Org. Chem.* **1994**, *59*, 3609–3615.

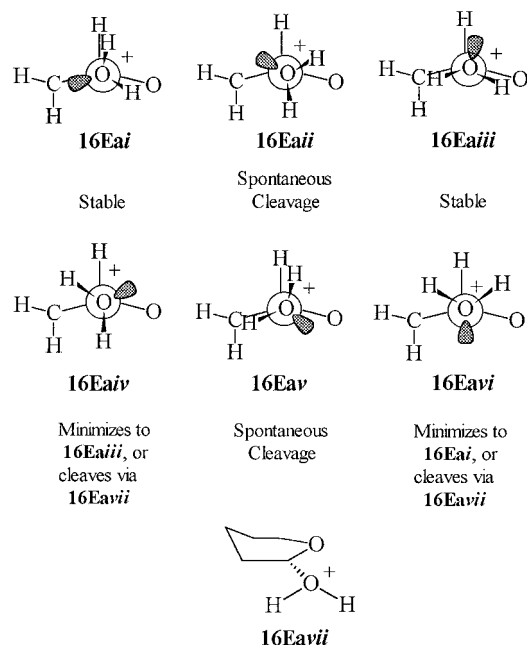
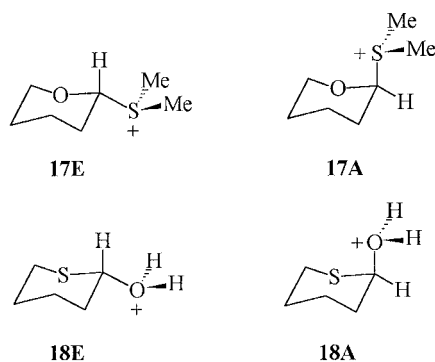
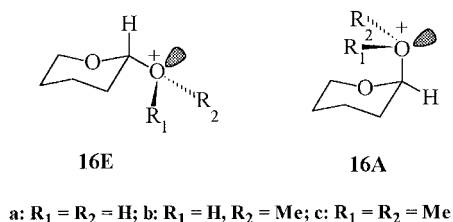


Figure 15. Six 60° rotomers for the protonated forms of equatorial 2-hydroxy-THP. **16Eavii** is an intermediate form produced by minimization of several rotomers (see text).

Chart 4



original rotomer reestablished manually, bond cleavage occurred through **16Eavii**. The energy difference is ca. 0.2 kcal/mol. The same pattern was found for both (*R*)- and (*S*)-forms of **16Eb**, with the exception that **16Ebvii** minimized to a stable form or cleaves via **15Ebvii** (Figure 16). In the axial compound **16Aa**, the only stable structure was **16Aai** (Chart 5). For the corresponding rotomer in the methoxy compound, the (*R*)-form was stable while the (*S*)-form cleaved. All forms of the equatorial and axial rotomers of the dimethylsulfonium compounds **16A,E** cleaved.

These results show that, at least in terms of the number of stable conformers, the equatorial is more stable than the axial conformation. The unprotonated hemiacetals and methyl acetals are subject to the anomeric effect with the axial form more stable than the equatorial, which was recently reaffirmed by Salzner and

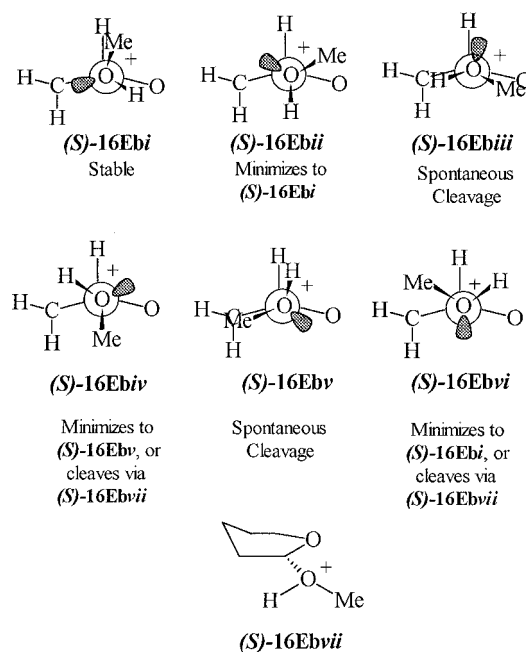
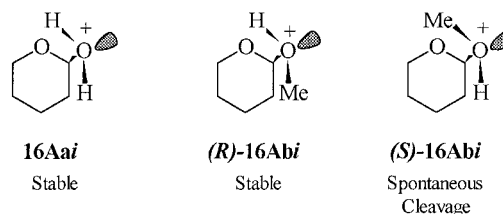


Figure 16. Six 60° rotomers for the protonated forms of equatorial 2-methoxy-THP. **16Ebvii** is an intermediate form produced by minimization of several rotomers (see text).

Chart 5



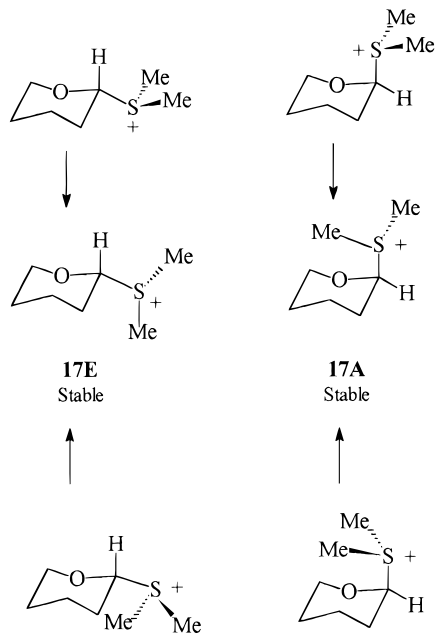
Schleyer¹⁸ with high-level *ab initio* calculations; our semiempirical methods (in PM3) reproduce the difference in ΔH_f found for various rotomers in the six-membered series. Because of the possibility of the so-called “reverse” anomeric effect—or as Perrin has pointed out recently,¹⁹ the lack of it in certain nitrogen compounds—we computed PM3 ΔH_f for the “generic” stable forms of **16Ea,b** and **16Aa,b** in which the anomeric carbon–oxygen bond length was constrained to 1.58 Å, the distance of this bond in the stable forms, and then minimized in MM2 and PM3. In **16a**, the axial isomer is more stable by 0.9 kcal/mol, but in **16b** the equatorial isomer is more stable by 0.4 kcal/mol. Thus there is no “reverse” anomeric effect for **16a**, but there is a slight reverse anomeric effect for **16b**, which matches the differences in reactivity measured by ΔH_R (Table 1) and the stability of the ion–dipole complexes (see below). Because the difference in energy is so small and because it is possible that Perrin’s explanation¹⁹ of electrostatic repulsion as a possible cause for the “reverse” anomeric is entirely reasonable, we do not wish to make too stringent a case for this effect to explain our results. An additional 18 cases have been examined computationally,²⁰ and the energy differences between equatorial and axial forms of various nitrogen,

(18) Salzner, U.; Schlyer, P. v. R. *J. Org. Chem.* **1994**, *59*, 2138–2155.

(19) Fabian, M. A.; Perrin, C. L.; Sinnott, M. L. *J. Am. Chem. Soc.* **1994**, *116*, 8398–8399. Perrin, C. L.; Armstrong, K. B.; Fabian, M. B. *J. Am. Chem. Soc.* **1994**, *116*, 715–722. Perrin, C. L.; Armstrong, K. B. *J. Am. Chem. Soc.* **1993**, *115*, 6825–6834.

(20) Buckley, N. Unpublished results.

Chart 6



oxygen, and sulfur compounds vary between 0.1 and 4.2 kcal/mol, with no apparent pattern in conformational preference.

The energy profiles for **16Ea**, **Aa** (Figure 13) were generated in PM3 as described for the 5-membered compounds. Both gave low but distinct transition states, with $\Delta H^\ddagger = 0.3$ kcal/mol for **16Aa** and 0.1 kcal/mol for **16Ea**. The ion-dipole complexes showed the same pattern, with the complex more stable for **16Ea** (-2.4 kcal/mol) than for **16Aa** (-1.4 kcal/mol).

Andrews et al.²¹ have published the results of an *ab initio* (6-31G*) study of the cleavage of **16Eb**, **Ab** that concentrated on the ring geometries of the starting structures and oxocarbenium ions. The rotomer dependence for cleavage was not addressed in their study. The convergence of three rotomers of **16Eb** to the half-sofa form **16Eb_{vii}** is in excellent agreement with their results for the equatorial compound, as are the structures of the oxocarbenium ions. We are greatly encouraged by this correspondence between high-level *ab initio* results and our (necessarily) cruder semiempirical results.

The effect of the leaving group is illustrated by the dimethylsulfonium substrates **17E** and **17A**, both of which minimize to a single stable structure regardless of the initial conformation (Chart 6). The thio-analogs **18Ea-c** and **18Aa-c** all spontaneously cleave regardless of the initial conformation (Chart 7). As found for the linear series, ΔH_R was much more exothermic for the thio analogs, with a slight preference for equatorial cleavage (Table 1).

(c) Ribofuranosides. These compounds (**19**, **20**; R = H, Me) show essentially the same behavior as found for the THF substrates with either water or methanol as the leaving group (Chart 8). The 2-deoxy compounds (**19aH** and **19aMe**) cleave from all rotomers, however. The protonated β -methylriboside **19cMe** is more stable than the protonated α -methyl riboside **20cMe** by 5.7 kcal/mol, a "reverse" anomeric effect. The α -methyl riboside cleavage reaction is more exothermic by the same amount,

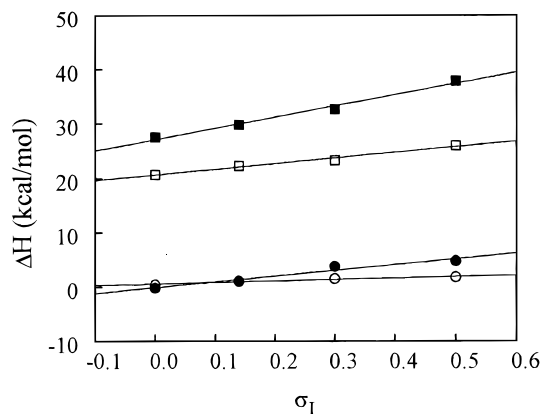


Figure 17. Plots of PM3 ΔH^\ddagger (open symbols) and ΔH_R (closed symbols) for C-O bond cleavage in **19a-d** with R = Me (circles) and the corresponding β -nicotinamide arabinosides (squares) from ref 17. The correlation coefficients are as follows: ■, $r = 0.994$; □, $r = 0.991$; ●, $r = 0.974$; ○, $r = 0.963$.

Chart 7

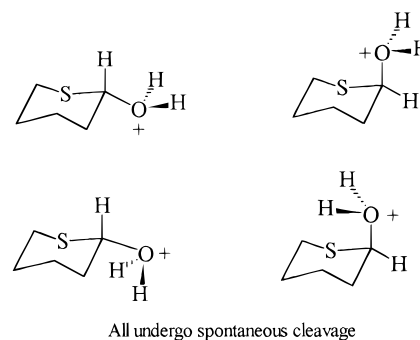
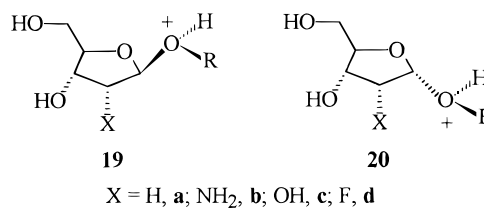


Chart 8



a consequence of the ground-state energies. In the 2-deoxy compounds **19aMe** and **20aMe**, however, the protonated α -methylriboside is more stable by 1.5 kcal/mol. These differences are not the result of the formation of hydrogen bonds as found for the hydroxy THF derivatives, however; no hydrogen bonds are formed in the most stable minimized forms, presumably because the rotomers necessary to form hydrogen bonds all have significant orbital-orbital repulsion.

The effects of substituents α to the anomeric carbon were examined. Plots of ΔH_R and ΔH^\ddagger vs σ_1 are linear for the cleavage of protonated 2-substituted (X = H, NH₂, OH, F) β -methylribosides **19a-dMe** (Figure 17), the same order as found for hydrolysis²² and gas-phase dissociation¹⁷ of β -nicotinamide arabinosides and hydrolysis of β -nicotinamide ribosides²³ bearing the same 2' substituents. The barriers to dissociation are low; for the 2'-F compound, which has the least stable ion-dipole complex and oxocarbenium ion, $\Delta H^\ddagger = 1.8$ kcal/mol.

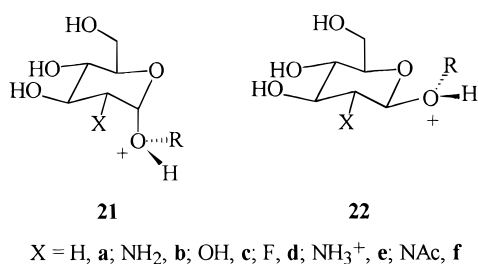
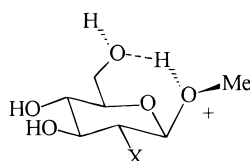
(21) Fraser-Reid, B.; Merritt, J. R.; Handlon, A. L.; Andrews, C. W. *Pure Appl. Chem.* **1993**, *65*, 779-786. Woods, J. R.; Andrews, C. W.; Bowen, J. P. *J. Am. Chem. Soc.* **1992**, *114*, 859-864.

(22) Handlon, A. L.; Oppenheimer, N. J. *J. Org. Chem.* **1991**, *56*, 5009-5010.

(23) Handlon, A. L.; Xu, C.; Müller-Steffner, H.-M.; Schuber, F.; Oppenheimer, N. J. *J. Am. Chem. Soc.* **1994**, *116*, 12087-12088.

Table 2. PM3 ΔH_f^\ddagger , ΔH^\ddagger , and ΔH_R (kcal/mol) for 2-Substituted α - and β -Methyl Glucosides

substituent		MeOH	ΔH_f^\ddagger	ΔH^\ddagger	ΔH_R
2'-deoxy	22a	α	-29.7	0	-3.9
	21a	β	-38.9	0.1	5.3
α -2'-amino	22b	α	-26.6	0.8	-1.6
	21b	β	-34.4	1.2	6.2
α -2'-hydroxy	22c	α	-74.2	1.0	4.2
	21c	β	-78.8	1.4	8.8
α -2'-fluoro	22d	α	-67.1	0	3.1
	21d	β	-75.8	2.2	12.8
β -2'-fluoro		α	-64.2	1.1	3.3
		β	-74.0	4.5	11.0

Chart 9**Chart 10**

Comparison with the results for the 2-substituted glucosides is given below. The ribosides are a well-behaved system.

(d) Methyl glucopyranosides. These compounds show the same rotamer dependence as found for the riboside/THF compounds (Chart 9). Unlike the ribosides, however, all β anomers of the protonated species (**22**) are more stable than the α anomers (**21**), which is the opposite of the trends found for the unprotonated compounds.¹⁸ As a consequence, reactions of all β anomers are more exothermic, often by substantial amounts (Table 2). The cause of this effect is the formation of hydrogen bonds between the protonated leaving group and the 5-oxygen (Chart 10), which, because of differences in ring geometry, is not possible in the β -methyl ribosides.

The effects of substituents α to the anomeric carbon (H, NH₂, OH, and F) is very much like that found for the β -methyl ribosides, with one exception. In the α -methyl glucopyranoside series (Figure 18), the points for the fluoro compounds are significantly off the correlation lines for the other three substituents, which is no doubt the result of a fluorine anomeric effect on the α compound that would stabilize the ground state and decrease both enthalpies (Chart 11).

For the β -methyl glucopyranosides, plots of ΔH_R and ΔH^\ddagger vs σ_I are linear (Figure 18), which parallels the results of Marshall²⁴ for the acid-catalyzed hydrolysis of the corresponding compounds. In fact, the correlation between $\log k_H^\ddagger$, the rate constant for the specific-acid catalyzed reaction, and the PM3 ΔH^\ddagger for Marshall's series of compounds is excellent (Figure 19), which provides

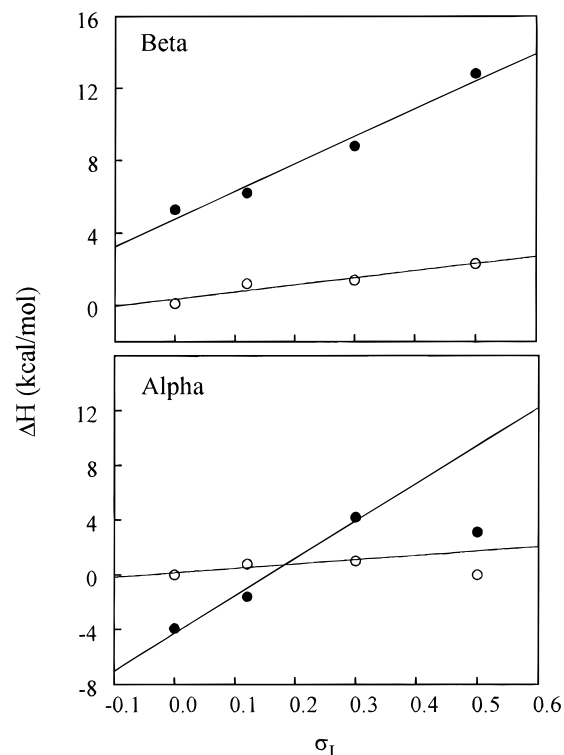
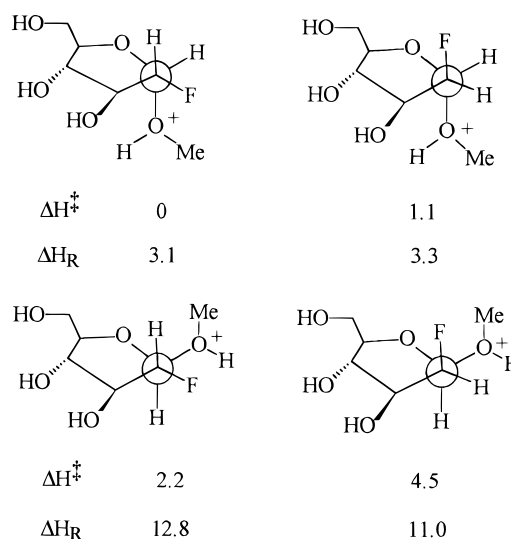


Figure 18. Plots of PM3 ΔH^\ddagger (○) and ΔH_R (●) for C–O bond cleavage in 2'-substituted β -methyl (**22a–d**) and α -methyl glucosides (**21a–d**). The points for **21d** are off the correlation line for the other substituents, presumably because of a fluorine anomeric effect. The correlation coefficients are as follows. β : ●, $r = 0.987$; ○, $r = 0.954$. α (ignoring F): ●, $r = 0.992$; ○, $r = 0.901$.

Chart 11

further confirmation that our methods reproduce accurately the relative energies involved in glycosyl bond cleavage, including the effects of substituents α to the reaction center.

(e) Oxygen vs Sulfur Substrates. Methyl 5-thiopyranosides undergo specific-acid catalyzed hydrolysis 10–15 fold faster than the corresponding oxygen compounds.^{1a,c} The corresponding ribosides show the same pattern of reactivity. This rate difference has been ascribed to increased proton affinity in the anomeric oxygen and not to a greater stability of the thio- over the oxocarbenium ion. In the companion paper,¹² we showed

(24) Marshall, R. D. *Nature* **1963**, *199*, 998–999.

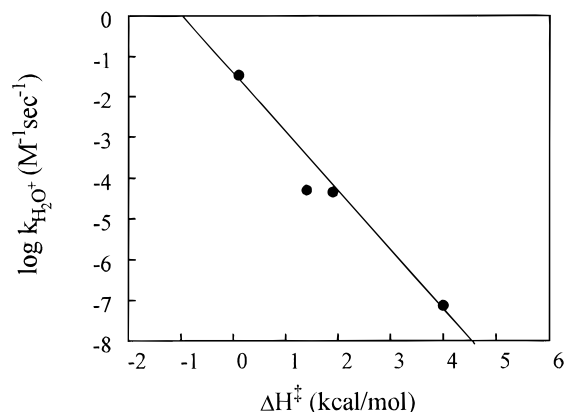


Figure 19. Plot of the log of the second-order rate constants for specific-acid-catalyzed hydrolysis at 25 °C of Marshall's series of 2-substituted β -methyl glucosides²⁴ vs the PM3 ΔH^\ddagger ($r = 0.980$). Left to right the points are for **21a,b,f,d**.

that $\text{HO}=\text{CH}_2^+$ was more stable than $\text{HS}=\text{CH}_2^+$ by 2.4 kcal/mol in PM3, but that $\text{MeS}=\text{CH}_2^+$ was more stable than $\text{MeO}=\text{CH}_2^+$ by 1.5 kcal/mol in PM3, with the same relative difference found in the experimental²⁵ and *ab initio*²⁶ (MP3/6-31G*) energies (see Table 2 of ref 12). For the RPy^+ compounds with $\text{R} = 2\text{-THF}$ or 2-tetrahydrothiophene, the AM1 ΔH^\ddagger was greater for the thio compound (by 1.4 kcal/mol), but ΔH_{R} was more exothermic for the thio compound (by 12.5 kcal/mol).

Both the 2-MeOTHP compound (**S-13Abvi**) and the 2-MeO-thio-THP compound (**S-17Abvi**) cleave with no barrier; the ion–dipole complex of the thio compound is 9.5 kcal/mol more stable than the ion–dipole complex of the oxo compound, and ΔH_{R} is 24.1 kcal/mol more exothermic for the thio compound, which shows that the thermodynamic driving force greatly favors the thiocarbenium ion. Unlike the pyridiniums, however, the ion–dipole complex for the thio-THP does not have a bridged structure (see Figure 2 in ref 12). These results suggest that, contrary to the commonly held view, in linear and cyclic secondary aliphatic systems there is substantial resonance participation of the sulfur with the cationic center. Indeed, between the ground-state and ion–dipole complex for (**S-13Abvi**) and (**S-17Abvi**), the change in charge on sulfur ($\delta q = 0.489$) is much greater than on oxygen ($\delta q = 0.183$), and the charge at the cationic center is actually more negative for the sulfur compound ($\delta q = -0.064$) than for the oxygen compound ($\delta q = 0.125$). This does not appear to be a computational artifact because correlations of semiempirical ΔH^\ddagger for cleavage of 4-MeS-ArCRR'X ($\text{R} = \text{R}' = \text{Me}$ or H ; $\text{R} = \text{H}$, $\text{R}' = \text{Me}$; $\text{X} = \text{H}_2\text{O}$, EtOH , MeOH , N_2) substrates fall where expected on correlation lines against either σ^+ or $\delta\Delta G^\circ$, a gas-phase stability scale based on *tert*-cumyl carbenium ions.²⁷ Our findings are also in accord with the recent *ab initio* results of Wiberg and Rablen²⁸ for thioformamide that showed greater resonance stabilization for $\text{H}_2\text{N}^+=\text{CS}^-$ than for $\text{H}_2\text{N}^+=\text{CO}^-$ and a substantial σ stabilization for the C–S bond that is largely Coulombic in character. The latter effect may account for the large difference in the

magnitude and sign of the charge on the cationic center between the sulfur and oxygen analogs in our series.

Alkyl glucosides in which the glycosidic oxygen is replaced by sulfur invariably react more slowly than the oxygen compounds; the effect is more dramatic in aryl glucosides.^{1a,c} This is clearly the result of the reduced proton affinity of SR compared to OR. Anti- and syn-periplanar effects are also important, however, and may be the dominant factor. This is shown by the finding that **13c** undergoes spontaneous cleavage regardless of stereochemistry, while **16** is stable. In **13c** there is a good LG with either or both anti- and syn-periplanar effects in any rotamer. The same effect is seen between the pyridinium and methyl ribosides, which is discussed below.

Comparison of Mechanisms. (a) A-1 vs A-2. The spontaneous cleavage, or cleavage with very low barriers, of protonated leaving groups in the linear and cyclic compounds is consistent with the A-1 mechanism that produces oxocarbenium ion intermediates, either as distinct species or elements of ion–dipole complexes. For linear pyridinium and dimethylanilinium substrates that show no distinct transition states, reactions with nucleophiles probably proceed through concerted displacement reactions. This is not the case for cyclic pyridinium compounds, which cleave to produce ion–dipole complexes.^{12,17}

Whether or not gas-phase results can be used to predict behavior in solution depends on the system. For instance, using Hammett and Brønsted plots of gas-phase relative rates and computational methods, we have shown that collisionally activated, gas-phase dissociation of benzyldimethylsulfoniums and pyridiniums occurs by direct dissociation and/or dissociation to ion–neutral complexes, respectively. The dimethylsulfoniums appear to undergo only direct dissociation, while the pyridiniums appear to react through a mixed mechanism involving both processes. The experimental results in water, however, show that (4-methoxybenzyl)dimethylsulfonium hydrolyzes by an $\text{S}_{\text{N}}1$ mechanism²⁹ but all other benzyldimethylsulfonium bearing less electron-donating groups react by solvent displacement,³⁰ and that all benzylpyridiniums react by direct solvent displacement.³¹ In solution, the entropy of solvation of the leaving group—or the lack of it for SMe_2 —appears to control the rate.^{29,31} Thus, the computational results accurately predict reactivity in the gas-phase but fail miserably for condensed-phase reactions.

On the other hand, the computed reaction profiles for β -nicotinamide arabinosides show dissociation to ion–dipole complexes, and both the experimental gas-phase and solution results are consistent with this mechanism.¹⁷ The arabinosides react faster in the gas-phase and in solution than either the dimethylsulfoniums or pyridiniums, which may reflect the increased stability of the ribosyl oxocarbenium ions compared with 4-substituted benzyl carbenium ions;^{8,17} certainly the calculated energies for the ion–dipole complexes show this difference.³² Moreover, the computed ΔH^\ddagger and ΔH_{R} correlate well with $\log k_{\text{H}_2\text{O}}$ and ΔG^\ddagger , ΔH^\ddagger , and ΔS^\ddagger for

(25) Taft, R. W.; Martin, R. H.; Lampe, F. W. *J. Am. Chem. Soc.* **1965**, *87*, 2490–2497.

(26) Apeloig, Y.; Karni, M. *J. Chem. Soc., Perkin Trans. 2* **1988**, 625–636.

(27) Taft, R. W.; Topsom, R. D. *Prog. Phys. Org. Chem.* **1987**, *16*, 2–83.

(28) Wiberg, K. B.; Rablen, P. R. *J. Am. Chem. Soc.* **1995**, *117*, 2201–2209.

(29) Buckley, N.; Oppenheimer, N. J. *J. Org. Chem.* **1994**, *59*, 5717–5723. Kevill, D. N.; Ismail, N. H. J.; D'Souza, M. J. *J. Org. Chem.* **1994**, *59*, 6303–6312.

(30) Friedberger, M. P.; Thornton, E. R. *J. Am. Chem. Soc.* **1976**, *98*, 2861–2865.

(31) Buckley, N.; Oppenheimer, N. J. *J. Org. Chem.* **1996**, *61*, 7360–7372.

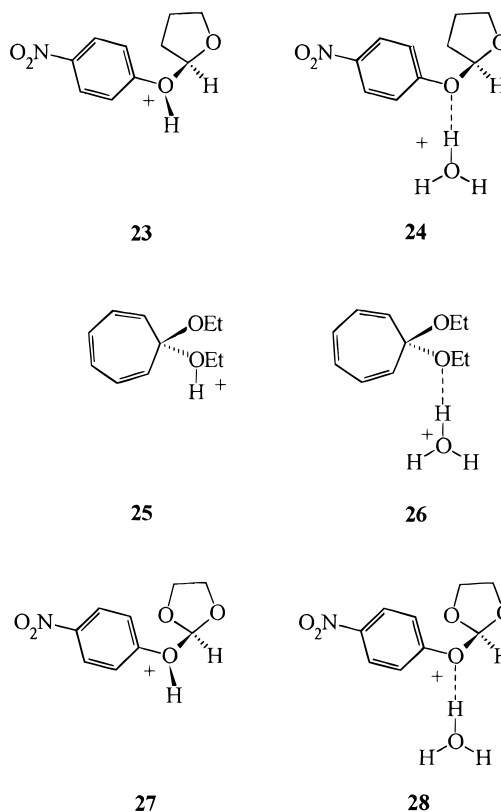
the solution reactions. For xylo- and glucopyranosyl pyridiniums, the computed ΔH^\ddagger correlates with ΔH^\ddagger and ΔS^\ddagger for the solution reactions.¹² Model studies with pyridinium LGs in 3-substituted THF substrates show an excellent correlation of the computed ΔH^\ddagger with σ_1 .²⁰ As shown above, the computed ΔH^\ddagger correlates very well with k_{H^+} for specific-acid-catalyzed hydrolysis of Marshall's series of 2-substituted methylglucosides (Figure 19), and there is an excellent correlation of the computed ΔH^\ddagger and ΔH_R with σ_1 for 2-substituted methyl ribosides (Figure 17) and for α and β methylglucosides (Figure 18). These results suggest that comparisons can be made for ribosides and glucosides between the gas and condensed phases.

They also suggest that there is no particular reason, on the basis of intrinsic energies, that ribosides and glucosides should not react by the same mechanism in solution. This is not in accord with the commonly-held view that the mechanism of hydrolysis is different for the two classes, a judgment made primarily from a consideration of ΔS^\ddagger values. Schlager and Long³³ have emphasized the dangers inherent in the use of ΔS^\ddagger values to differentiate among mechanisms; nonetheless, for compounds of similar structures and reactions of similar energies, if used with caution and with other supporting evidence, ΔS^\ddagger is a reasonable criterion. For the methyl pyranosides, ΔS^\ddagger are high and positive,^{1a} which is consistent with rate-limiting bond cleavage of a preprotonated substrate—the A-1 mechanism. Methyl furanosides, however, invariably react with negative values of ΔS^\ddagger , which has led some workers to suggest that the protonated alcohol moiety is displaced by water in the A-2 mechanism.¹ A rate analysis using Bunnett's ω -scale supports the A-2 mechanism for furanosides.³⁴

For the pyridinium substrates, however, ΔS^\ddagger values are high and positive for both β -nicotinamide ribosyl and arabinosyl compounds ($\Delta S^\ddagger = 1.6$ – 13.2 gibbs/mol) and β -pyridinium glucosyl, xylosyl, and galactosyl compounds ($\Delta S^\ddagger = 15$ – 31 gibbs/mol). Shuber³⁵ has shown that hydrolysis of a series of NAD⁺ analogs with different pyridine LGs has a β_{LG} value of -1.11 . We have shown that the ribosyl oxocarbenium ion is more stable in the gas phase than the 4-methoxybenzyl carbenium ion,³¹ a species known to be a solvent-equilibrated intermediate in solvolysis reactions of neutral³⁶ and positively-charged substrates.²⁹ Taken with the computational profiles, gas-phase results, and other correlations, the entropy results are consistent with a common dissociative mechanism for both classes of compounds. As shown below, it is possible that the entropy differences reflect the mode of proton transfer and not a change in mechanism from direct dissociation to displacement of the protonated LG by water.

(b) Specific- vs General-Acid Catalysis. As Handlon and Oppenheimer²² have pointed out, one difference between the pyridinium substrates and methyl ribosides and glucosides is that the former bear a formal positive

Chart 12



charge in the ground state, while the latter must be protonated before reaction can occur. The compounds studied here do not undergo general-acid catalysis (or the so-called A_{SE}2 mechanism) in solution, so the reactive intermediate must form in a preequilibrium $ROR' + H_3O^+ \rightleftharpoons ROR'H^+ + H_2O$; for the simple A-1 mechanism, dissociation of the protonated intermediate (k_2) is rate-limiting. In this case, $k_{obsd} = K_a k_2$. Cordes and Bull^{1b} have pointed out that reasonable values of k_2 can be calculated using k_{obsd} and measured values of pK_a for acetals.

For simple acetals, the proton affinity is affected by either R or R'. For R containing the potential oxocarbenium ion, the orientation of OR' relative to the α oxygen affects the proton affinity of the LG because of $n\sigma^*$ interactions, an idea first suggested by Deslongchamps¹⁶ and confirmed by Andrews et al.¹⁴ in their study of **6**. Our results support this contention. Inductive effects on the R' group also affect proton affinity. Alkyl groups are much more basic (pK_a MeOH = 15.5) than phenols (pK_a 4-NO₂-phenol = 7.2), yet compounds such as **23** and **25** undergo general-acid catalyzed and "spontaneous" hydrolysis reactions (Chart 12). Invoking Jencks's "libido rule", which states (roughly) that general acid catalysis would be expected for systems in which the pK of the catalyst is intermediate between the site being protonated and the final product,³⁷ Cordes and Bull^{1b} point out that acetals (or ketals or orthoesters) with phenol LGs would be expected to undergo general-acid catalysis. They also argue that within a series, it would be expected that substrates containing potentially stable carbenium ions should undergo general acid catalysis in an order that depends on carbenium ion stability.

We attempted to model this effect with hydronium as the general acid in **24**, **26**, and **28**, all of which are known

(32) One of us (N.B.) has found that the PM3 ΔH^\ddagger for the reaction $R^+ + R'OH \rightarrow ROHR^+$ and ΔH_R for the reverse reaction give excellent correlations with the respective measured rate constants for R = α -phenylethyl, *tert*-cumyl, 4,4,5,5-tetramethyldioxolane, and diethoxymethylmethyl carbenium ions. (Buckley, N. Unpublished results.)

(33) Schaleger, L. L.; Long, F. A. *Adv. Phys. Org. Chem.* **1963**, *1*, 1–34.

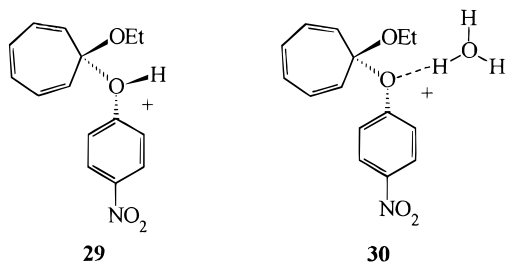
(34) Bunnett, J. F. *J. Am. Chem. Soc.* **1961**, *83*, 4978–4983.

(35) Tarnus, C.; Schuber, F. *Bioorg. Chem.* **1987**, *15*, 31–42. Tarnus, C.; Muller, H. M.; Schuber, F. *Bioorg. Chem.* **1988**, *16*, 38–51.

(36) Amyes, T. L.; Richard, J. P. *J. Am. Chem. Soc.* **1990**, *112*, 9507–9512.

(37) Jencks, W. P. *Chem. Rev.* **1972**, *72*, 705–718.

Chart 13



to undergo general-acid catalysis in solution (Chart 12). With the RO- -H- -⁺OH₂ bond constrained to linearity, **24** and **26** were stable, but **28** underwent spontaneous cleavage. In **24** and **26**, the proton remained bound to the water, which prevents cleavage. Attempts to reduce the proton affinity of the water oxygen by hydrogen bonding two waters to the remaining hydronium protons in **26** did not alter the reaction profile, even in a structure with an anti-periplanar orbital interaction. This is of course a *very* crude approximation of solvent stabilization. In **28**, starting with a hydronium structure with three equal H-O bond lengths of 0.96 Å and an H-LG oxygen bond length of 1.8 Å, minimization leads to transfer of the proton from the water to the phenol oxygen with a concomitant increase in the length of the reaction coordinate bond. (Note that if the phenol in **23** and **24** is replaced by OEt, the preprotonated compound undergoes spontaneous cleavage, but the hydronium-bound species is stable.)

These results show that the LG is more important than the carbenium ion for this effect. The order is counter-intuitive, however, because values of ΔH_R for reaction of **23**, **27**, and **25**, all of which undergo spontaneous cleavage upon minimization, are -13.1, -14.6, and -26.2 kcal/mol, respectively, with tropyllium heavily favored. In fact, the relative rate for hydration of the ethoxytropyllium carbenium ion derived from **25** and the dioxolane oxocarbenium ion³⁸ derived from **27** is 10^{11} in favor of tropyllium! From the trends in this series, we can predict that **29** and **30** (Chart 13) will have the highest ΔH_R and will undergo hydronium ion general-acid catalysis, respectively, which in the event are the trends found: ΔH_R for **29** = -38.2 kcal/mol and **30** cleaves synchronously with proton transfer.

A long-standing conundrum in the understanding of the mechanism of general-acid catalysis in these compounds is whether proton transfer from the general acid to the substrate is rate limiting or whether proton transfer and bond cleavage occur synchronously.^{1a} These effects are difficult if not impossible to determine from kinetics. For instance, Schowen³⁹ has shown that kinetic isotope effects cannot be used to differentiate among mechanisms. While this is the rawest kind of speculation, the solution results—all general-acid catalyzed—and our computational results—no proton transfer from hydronium in **24** and **26** and proton transfer with concerted bond cleavage in **28** and **30**—suggest that proton transfer is rate limiting for **24** and **26** and that proton transfer

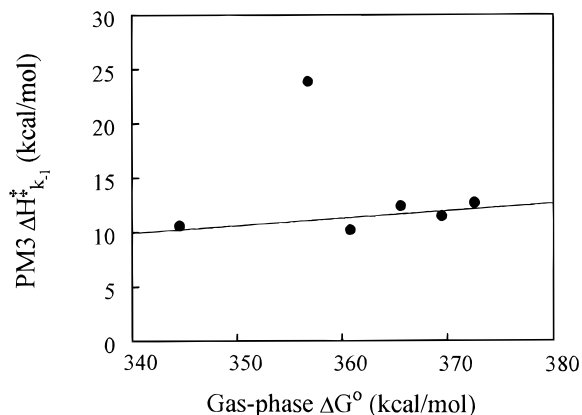


Figure 20. Plot of the PM3 ΔH_{k-1}^\ddagger (kcal/mol), the difference between the ground-state and ion-dipole complex structures that is also ΔH^\ddagger for the addition of alcohols to the carbenium ion, vs the absolute gas-phase ΔG° (kcal/mol) for the alcohols (from Bartmess, J. E.; Scott, J. A.; McIver, R. T., Jr. *J. Am. Chem. Soc.* **1979**, *101*, 6046–6056). The value of ΔG° for propargyl alcohol was estimated from a plot of ΔG° vs pK_a of the other alcohols ($r = 0.994$). Left to right the points are for phenol, TFE, propargyl alcohol, 2-methoxyethanol, ethanol, and methanol.

and bond cleavage are synchronous for **28** and **30**. Thus, the presence of either an LG with a low basicity (**24**) or an excellent carbenium ion (**26**) is not sufficient to allow concerted bond cleavage and proton transfer, which will occur only when both are present (**28** and **30**).

Jensen and Wuhrman⁴⁰ have reported that in a series of compounds equivalent to **16A** with various alcohol LGs (ROH = MeOH, EtOH, 2-MeO-EtOH, propargyl alcohol, 2-chloroethanol, 2,2,2-trifluoroethanol (TFE)), the propargyl and TFE substrates undergo general-acid catalysis; the second-order rate constant for HOAc catalysis is ca. 10^{-5} lower than the hydronium rate constant, so the effect is not large and difficult to detect above small salt effects. We have examined this series and find that no substrate cleaves with hydronium as a general acid. An interesting finding, however, is that the energies (in kcal/mol) of the ion-dipole complexes relative to the starting structures, which were given the same stereochemistry as (**S**)-**17Abvi**, for specific-acid-catalyzed cleavage have similar values (MeOH = -12.7; EtOH = -11.5; MeO-CH₂CH₂, -12.4; propargyl = -10.2; phenol = -10.6) except for the TFE compound (-23.9). (The equatorial compounds show the same trends.) The ion-dipole complexes for the “normal” alcohols all have the structure R⁺- -OHR’, while the TFE ion-dipole complex has the structure R⁺- -F₃CCH₂OH. Such a dipolar structure has been suggested by Richard and Jencks⁴¹ for an α -phenylethyl carbenium ion-TFE encounter complex. One of us (N.B.) has found this structure to be important for carbenium ion combination reactions of benzyl, α -phenylethyl, and *tert*-cumyl carbenium ions.³² While the complex would not affect the bond-breaking step, it would have an enormous effect on the recombination reaction, increasing the ΔH_{k-1}^\ddagger by ca. 12 kcal/mol based on the expected value obtained by extrapolation of the plot shown in Figure 20.

(c) Aryloxy- vs Pyridinium THF Substrates. While solution data are not available to allow a strict compari-

(38) The rate constant for the hydration of the ethoxytropyllium carbenium ion is from: McClelland, R. A.; Ahmad, M. *J. Am. Chem. Soc.* **1978**, *100*, 7027–7031. The rate constant for hydration of the unsubstituted dioxolane oxocarbenium ion ($1.7 \times 10^9 \text{ M}^{-1} \text{ s}^{-1}$) was estimated from ratios of rate constants for the 2-Me 3,3,4,4-protio- and tetramethyldioxolanes and the 2-H 3,3,4,4-tetramethyldioxolane oxocarbenium ions: Steenken, S.; McClelland, R. A. *J. Am. Chem. Soc.* **1989**, *111*, 4967–4973.

(39) Schowen, R. L. *Prog. Phys. Org. Chem.* **1972**, *9*, 275–302.

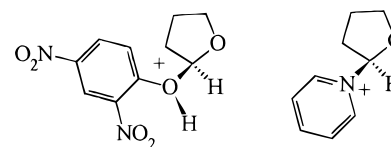
(40) Jensen, J. L.; Wuhrman, W. B. *J. Org. Chem.* **1983**, *48*, 4686–4691.

(41) Richard, J. P.; Jencks, W. P. *J. Am. Chem. Soc.* **1984**, *106*, 1373–1383.

son, the relative rates between a protonated phenol and a pyridine as LGs can be obtained by crude extrapolation of Lathi's data⁴² for the specific-acid-catalyzed hydrolysis of 2-(aryloxy)-THF substrates and from Handlon's rate constant²² for the hydrolysis of β -nicotinamide 2'-deoxyriboside. We estimate that **31** (pK_a LG = 4.1) hydrolyzes $\sim 3.6 \times 10^3$ faster than β -nicotinamide 2'-deoxyriboside (pK_a LG = 3.33) at 37 °C. This large difference is also reflected in the energies for bond cleavage of **31** and **32** (Chart 14), relatively simple computational systems with LGs of approximately the same pK_a . (The AM1 energies for **32** were reported in the companion paper,¹² and the energies for **31** were calculated in this method.) The values $\Delta\Delta H^\ddagger \sim 22.7$ kcal/mol and $\Delta\Delta H_R = 43.0$ kcal/mol show the same trends found in the crude comparison of water rate constants. It is readily apparent that the difference is the result of the anti- or syn-periplanar interactions of the LG and ring oxygens in **31** that are not available in **32**. Thus, while the gas-phase mechanisms are the same—dissociative cleavage to a stable ion–dipole complex—the driving forces and energies are clearly different and favor the phenol over the pyridinium. Here, too, however, the solution ΔS^\ddagger have different signs. Lathi⁴² found $\Delta S^\ddagger = -6.4 \pm 0.7$ gibbs/

(42) Lahti, M.; Lindström, R.; Lönnberg, H. *J. Chem. Soc., Perkin Trans. 2* **1989**, 603–605. The rate constant for the specific-acid catalyzed hydrolysis of **31** was estimated from the Hammett ρ value of -0.97 for reaction at 25 °C; this was extrapolated to 35 °C by a simple ratio with the respective rate constants for 2-(3-(chloroaryl)-oxy)THF, which is based on the reasonable assumption that the Eyring plots for these substrates have the same slopes.

Chart 14



	31	32
pK_a LG	4.09	5.25
ΔH^\ddagger (kcal/mol)	~ 0	22.7
ΔH_R (kcal/mol)	-8.9	34.1

mol for 2-(4-chlorophenoxy)-THF, while Handlon⁴³ found $\Delta S^\ddagger = 9.5 \pm 2.5$ gibbs/mol for β -nicotinamide 2'-deoxyriboside. Given this profile, it is doubtful that **31** reacts through an A-2 mechanism, with the negative ΔS^\ddagger arising from direct displacement of the LG by water. It seems more probable, given the results for **23–30**, that the negative ΔS^\ddagger arises because the activated complex is organized from the substrate and hydronium in a mechanism in which proton transfer is rate limiting.

Acknowledgment. Supported in part by NIH Grant No. GM-22982.

JO960748T

(43) Handlon, A. L. Ph.D. Dissertation, University of California, San Francisco, 1991.